PHYSICAL REVIEW E **68**, 035401(R) (2003)

Polarization of wave modes in a two-dimensional hexagonal lattice using a complex (dusty) plasma

S. Zhdanov, S. Nunomura, D. Samsonov, and G. Morfill
CIPS, Max-Planck-Institut für Extraterrestrische Physik, D-85740 Garching, Germany
(Received 12 June 2003; published 9 September 2003)

Wave spectra corresponding to the random particle motion in a monolayer Yukawa crystal were studied for various directions of propagation. It was found that there are two wave modes with a polarization alternating between the longitudinal and transverse. In the long-wavelength regime, the modes became purely longitudinal and transverse as was known before. In the short-wavelength regime the spectra strongly depended on the wavelength and the direction of propagation. The results obtained from the experiment, theory, and simulation agreed well with each other.

DOI: 10.1103/PhysRevE.68.035401 PACS number(s): 52.27.Lw, 52.35.Fp, 46.40.−f

Complex (dusty) plasmas consist of submicron to micron sized particles immersed into an electron-ion plasma. The particles charge up and interact strongly with each other. When their potential interaction energy significantly exceeds their kinetic energy, complex plasmas can form ordered structures or exist in a crystalline state [1–4]. Such crystalline structures can be easily observed with a video camera and used as a macroscopic model system to study waves, phase transitions, and other microscopic phenomena at a kinetic level [5].

Waves in a two-dimensional (2D) Yukawa lattice were analyzed theoretically in Refs. [6–8]. It was found that there are two wave modes: longitudinal and transverse. These modes were observed experimentally in Refs. [9,10] using laser excitation. This method, however, produced only waves with long wavelengths. Observing naturally excited thermal motion of the particles allows measurements of the dispersion relations for short wavelengths [11].

The dispersion relations in Refs. [9–11] were measured only for the waves propagating along the main crystalline axes. While the elastic and long-wavelength properties of a hexagonal lattice are isotropic, it is known that the short-wavelength waves are strongly anisotropic [7,8,12]. In this paper we report results on the dispersion relations and polarization of the thermal waves for different directions of propagation in a hexagonal Yukawa lattice experimentally, theoretically, and using a simulation.

The experiments are performed in a capacitively coupled rf discharge (Fig. 1), which is similar to the apparatus of Ref. [13]. A plasma is generated by applying a rf power of 2 W at 13.56 MHz to the lower rf electrode. An argon gas flow is regulated at a rate of 1.8 SCCM (cubic centimeter per minute at STP) to achieve the working gas pressure of 1.0 Pa in the chamber.

We introduce plastic microspheres with the diameter of 8.9 ± 0.1 μm into the plasma. These particles charge negatively in the plasma and levitate in the electric field of the plasma sheath above the lower electrode. They are confined radially in a bowl-shaped potential formed by a rim on the outer edge of the electrode. Once the particles are cooled down by the gas drag, they form a monolayer hexagonal lattice. The particle suspension is ≈ 7 cm in diameter and levitates at a height of $\simeq 9$ mm above the lower electrode. The mean particle separation a is 780 μm.

To observe the particle motion, the lattice is illuminated by a horizontal thin (0.2–0.3 mm) sheet of laser light and viewed from the top window. The images from a digital video camera are recorded for several seconds at 33 frames/s. Using an image processing software, the particle positions are identified and traced from one frame to the next. The particle velocities are calculated from their displacement in two consecutive frames.

In our crystal, the particles always exhibit random motion around their equilibrium positions. The fluctuation amplitude is typically a few percent of the particle separation a. The particle velocities have a Maxwellian distribution. We determine the crystal kinetic temperature T from the width of this distribution to be 0.055 eV.

In order to analyze the particle random motion we Fourier transform the particle velocity field $v(x,t)$ both in the direc-

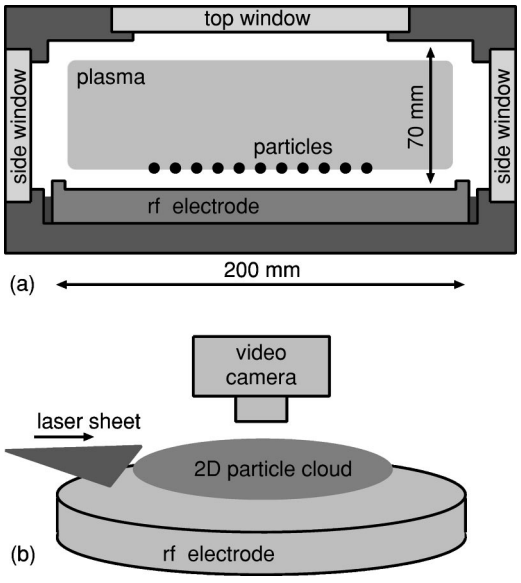

FIG. 1. Sketch of apparatus. (a) Side view. The aluminum vacuum chamber is equipped with a rf electrode 200 mm in diameter. The rf voltage is applied between the electrode and the grounded chamber creating a plasma. Spherical particles charge negatively and form a monolayer levitating in the plasma sheath above the lower electrode. The optical access is provided by four side windows and a top window. (b) Oblique view. The particles are illuminated with a sheet of a doubled Nd:YAG (yttrium aluminum garnet) laser (532 nm) and viewed from top with a video camera.

 ©2003 The American Physical Society

tion of the wave propagation x and in time t, producing the phonon spectra

$$\mathbf{V}_{\mathbf{k},\omega}=\frac{2}{L_0T_0}\sum_{i=0}^{n_l}\sum_{j=0}^{n_t}\mathbf{v}(\mathbf{x},t)\exp(\mathbf{k}\cdot\mathbf{x}-\omega t)\Delta x\Delta t, \quad (1)$$

where $\mathbf{k}$ and ω are the wave number and the angular frequency of the wave, n_l and n_t are the numbers of data points in space and time, L_0 and T_0 are the lengths of the field of view and the recording period, respectively, and Δx and Δt are the distances between the data points and the time interval. The wave polarization is taken into account by discriminating between the longitudinal $v_{\parallel}(x,t)$ and transverse $v_{\perp}(x,t)$ velocities, which are the velocity components parallel and perpendicular to the direction of propagation. We measure the phonon spectra at various directions of the wave propagation θ with respect to the crystal lattice by suitably selecting the direction of the x axis.

Formula (1) takes into account that our data (particle positions) are randomly spaced, and therefore the resolution of this technique is determined by the resolution and the frame rate of the camera and tracing software, not by the particle separation.

From the Fourier amplitude of the particle velocity $V_{\mathbf{k},\omega}$, we calculate the density of phonon energy $E_{\mathbf{k},\omega}$. In order to get the absolute value of the energy it should be normalized by the volume in $(\mathbf{k},\omega,\theta)$ space. We also normalize the phonon energy by the particle kinetic temperature T,

$$E_{\mathbf{k},\omega}=mV_{\mathbf{k},\omega}^2/2k\,\delta\theta\,\delta k\,\delta\omega k_{\mathrm{B}}T, \quad (2)$$

where $\delta\theta$, δk, and $\delta\omega$ are the resolutions of our Fourier method in θ, $\mathbf{k}$, and ω, respectively, and k_{B} is the Boltzmann constant. The normalization factor is constant, $k\,\delta\theta\,\delta k\,\delta\omega=0.0597\ \mathrm{mm}^{-2}\,\mathrm{s}^{-1}$, under our experimental conditions.

The *theoretical model* is based on the 2D equations of motion

$$m\ddot{\mathbf{r}}_s=\mathbf{f}_s^{fr}+\mathbf{f}_s^{conf}+\mathbf{f}_s^{int}+\mathbf{f}_s^{exc},$$

$$\mathbf{f}_s^{fr}=-m\nu\dot{\mathbf{r}}_s, \quad \mathbf{f}_s^{conf}=-m\Omega_{conf}^2\mathbf{r}_s,$$

$$\mathbf{f}_s^{int}=-\nabla U_s, \quad U_s=Q^2\sum_{j\neq s}r_{sj}^{-1}\exp(-r_{sj}/\lambda_D), \quad (3)$$

where m is the mass of the particles, $\mathbf{r}$ is the particle coordinate with the subscripts s and j denoting different particles, $\mathbf{f}_s^{fr}$ is the friction due to collisions with neutrals (Epstein drag), $\mathbf{f}_s^{conf}$ is the confinement force due to a parabolic potential, $\mathbf{f}_s^{int}$ is the grain-grain interaction force, $\mathbf{f}_s^{exc}$ is the external excitation force, ν is the neutral damping rate, Ω_{conf} is the confinement parameter of the parabolic well, U_s is the grain-grain interaction screened Coulomb (Yukawa) potential energy, Q is the particle charge, $r_{sj}=|\mathbf{r}_s-\mathbf{r}_j|$ is the intergrain distance, and λ_D is the screening length.

In the absence of external excitation forces, the lattice would relax to an equilibrium state and cool down due to the neutral drag. We assume that $\mathbf{f}_s^{exc}$ is random and of a small amplitude, so that it causes a very small displacement of the particle to which it is applied. This assumption allows us to obtain an analytical solution for the polarization of two different branches of the dispersion relation.

In order to solve Eqs. (3) we introduce $\mathbf{r}_s=\mathbf{R}_s+\delta\mathbf{r}_s$, where $\delta\mathbf{r}_s$ is a small deviation from the static equilibrium position of the particle $\mathbf{R}_s$. We then solve the linearized system of equations for harmonic motion $\delta\mathbf{r}_s=\boldsymbol{\xi}_{\mathbf{k},\omega}\exp(i\mathbf{k}\cdot\mathbf{R}_s-i\omega t)$ obtaining the equations for the phonon spectrum:

$$\omega(\omega+i\nu)\boldsymbol{\xi}_{\mathbf{k},\omega}=\hat{\mathbf{D}}_{\mathbf{k},\omega}\boldsymbol{\xi}_{\mathbf{k},\omega}+\Omega_{conf}^2\boldsymbol{\xi}_{\mathbf{k},\omega}-(\mathbf{f}/m)_{\mathbf{k},\omega}^{exc}, \quad (4)$$

where $\hat{\mathbf{D}}_{\mathbf{k},\omega}$ is the dynamics matrix which describes the linear response of a Yukawa system and $(\mathbf{f}/m)_{\mathbf{k},\omega}^{exc}$ is the acceleration produced by the excitation force. The components of $\hat{\mathbf{D}}_{\mathbf{k},\omega}$ can be written as

$$D_{\mathbf{k},\omega}^{xx}=\alpha-\beta, \quad D_{\mathbf{k},\omega}^{yy}=\alpha+\beta, \quad D_{\mathbf{k},\omega}^{xy}=D_{\mathbf{k},\omega}^{yx}=\gamma,$$

where the coefficients α, β, and γ are

$$\alpha=\Omega_*^2\sum e^{-K}K_1\sin^2(\mathbf{k}\cdot\mathbf{R}/2),$$

$$\beta=\Omega_*^2\sum e^{-K}K_3[(R_y^2-R_x^2)/R^2]\sin^2(\mathbf{k}\cdot\mathbf{R}/2),$$

$$\gamma=\Omega_*^2\sum e^{-K}K_3[2R_xR_y/R^2]\sin^2(\mathbf{k}\cdot\mathbf{R}/2), \quad (5)$$

with the parameters

$$\Omega_*^2=Q^2/(m\lambda_D^3), \quad K=R/\lambda_D,$$

$$K_1=K^{-3}+K^{-2}+K^{-1}, \quad K_3=3K^{-3}+3K^{-2}+K^{-1}.$$

The sums in Eqs. (5) are calculated over the indices p and q which represent the particle positions (R_x,R_y) in an infinite hexagonal lattice

$$R_x=ap\sqrt{3}/2, \quad R_y=a(q+p/2), \quad R=a\sqrt{p^2+q^2+pq},$$

where a is the particle separation.

The general solution $\boldsymbol{\xi}_{\mathbf{k},\omega}$ of Eqs. (4) is

$$\boldsymbol{\xi}_{\mathbf{k},\omega}=\sum_{j=1,2}\mathbf{e}_{\mathbf{k},\omega}^{(j)}[\mathbf{e}_{\mathbf{k},\omega}^{(j)}\cdot(\mathbf{f}/m)_{\mathbf{k},\omega}^{(j)}]G_j, \quad (6)$$

where $G_{1,2}=(\Omega_{1,2}^2+\Omega_{conf}^2-\omega^2-i\nu\omega)^{-1}$, and two pairs of eigenvectors $\mathbf{e}_{\mathbf{k},\omega}^{(1,2)}$ and eigenvalues $\Omega_{1,2}^2$ of the dynamic matrix $\hat{\mathbf{D}}_{\mathbf{k},\omega}$ represent two different branches of the dispersion relations. The dependencies $\Omega_{1,2}(\mathbf{k})$ are our theoretical dispersion relations. They do not take into account Ω_{conf} and ν, which are negligible in the experiment.

Making a transformation from Cartesian (β,γ) to cylindrical (ρ,ϕ) coordinates we get $\beta=\rho\cos\phi$, $\gamma=\rho\sin\phi$, and therefore

$$\mathbf{e}_{\mathbf{k},\omega}^{(1)}=(\sin\phi/2,\cos\phi/2), \quad \Omega_1^2=\alpha+\rho,$$

$$\mathbf{e}_{\mathbf{k},\omega}^{(2)}=(\cos\phi/2,-\sin\phi/2), \quad \Omega_2^2=\alpha-\rho.$$

Ω_1 corresponds to the high frequency branch if the branches are not degenerate. The eigenvectors determine the polarization of the dispersion branches. They are neither parallel nor

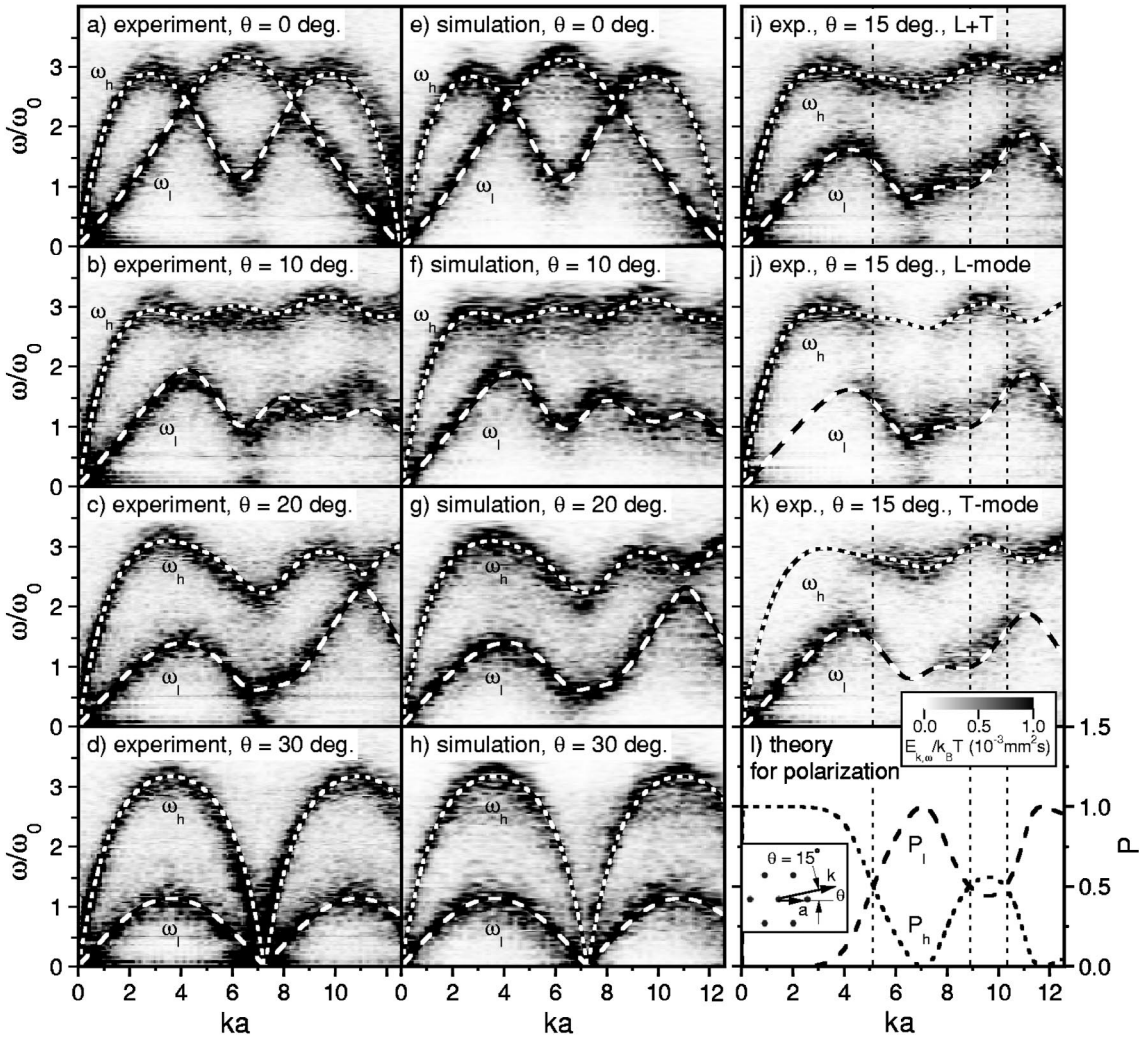

FIG. 2. Phonon spectra of thermally excited waves in the first and second Brillouin zone at different angles of propagation, (a)–(d) experiment and (e)–(h) simulation. The theoretical dispersion relations are superposed: dotted line (high frequency mode ω_h) and dashed line (low frequency mode ω_l). The normalization constant $\omega_0 = Q/\sqrt{ma^3}$. The dispersion relation is periodic for 0° and 30° but it is aperiodic in general. (i) Phonon spectra of the waves propagating at 15° measured experimentally. The high and low frequency branches have mixed longitudinal (j) and transverse (k) polarization. (l) Polarization of the high frequency (P_h) and low frequency (P_l) modes predicted by the theory. At low wave numbers (long wavelengths) the high frequency mode is purely longitudinal ($P_n = 1$), and the low frequency mode is purely transverse ($P_l = 0$). At an arbitrary wave number the modes have mixed polarization.

perpendicular to **k** and their orientation changes with **k**. Note that the eigenvalues $\Omega_{1,2}^2 > 0$ and therefore the lattice is stable.

The polarization P is calculated from the general solution [Eq. (6)] by taking the longitudinal and transverse components and averaging their absolute values over the orientation of the random excitation force:

$$\langle |\vec{\xi}_{\mathbf{k},\omega}^{long}|^2 \rangle = |(\mathbf{f}/m)_{\mathbf{k},\omega}^{exc}|^2 [P|G_1|^2 + (1-P)|G_2|^2]/2,$$

$$\langle |\vec{\xi}_{\mathbf{k},\omega}^{trans}|^2 \rangle = |(\mathbf{f}/m)_{\mathbf{k},\omega}^{exc}|^2 [(1-P)|G_1|^2 + P|G_2|^2]/2,$$

where $P = (\mathbf{e}_{\mathbf{k},\omega}^{(1)} \mathbf{k}/k)^2$ is the polarization of the first branch and $(1-P)$ of the second. The polarization changes in the range between 0 and 1. The zero value corresponds to the purely transverse polarization, while the unity corresponds to the purely longitudinal wave.

These results are for an infinite lattice. However they are applicable for a finite cluster if $R_0 \gg \lambda_\nu$, where R_0 is the cluster radius and $\lambda_\nu \propto 1/\nu$ is the damping length. The damping length is smaller for shorter waves making them more local.

We also modeled the 2D complex plasma using a *molecular dynamics simulation*. The method is based on the 2D equations of motion [Eqs. (3)]. They are made dimensionless using parameters λ_D and $T_* = \sqrt{m\lambda_D^3/Q^2}$ and solved with a sixth-order Runge-Kutta integration method taking into account the interaction of every particle with every other one. A 2D cloud (721 particles) is placed in a confinement potential with the confinement parameter $\Omega_{conf} = 2\ \mathrm{s}^{-1}$. We assume a particle charge $Q = 17000e$, a screening parameter $\kappa \equiv a/\lambda_D = 1$, and a damping constant $\gamma = 1.37\ \mathrm{s}^{-1}$. The parameters of the simulation are selected to match those of the experiment. The lattice is equilibrated by running the code

for a sufficient number of time steps, and then the random excitation force is applied. The phonon spectra are obtained for the central homogeneous part of the lattice with the method described above [Eqs. (1) and (2)]. The lattice kinetic temperature of 0.058 eV, obtained in the simulation, closely matches the experimental value of 0.055 eV.

We now discuss our measurements, the theory outlined above, and the simulations. The *experimental phonon spectra* of the thermally excited waves are shown in gray scale in Figs. 2(a)–(d) at different propagation angles. Figures 2(e)–(h) show the corresponding simulation results. The dashed lines represent the theoretical dispersion relations. The propagation angle θ is measured with respect to one of the main crystal axes [lattice inset in Fig. 2(l)]. The hexagonal lattice has two main axes at $\theta=0°$ and at $\theta=30°$. The angles in this range cover all possible directions in the crystal due to its symmetry.

The spectra in Fig. 2 are plotted for the wave numbers k extending into the second Brillouin zone, which corresponds to wavelengths smaller than the particle separation a. This would not make any sense for a linear chain, which can only sustain waves with wavelengths longer than $2a$, meaning that the spectra with $ka>\pi$ are artifacts of the Fourier transformation and repeat periodically. This is different for a 2D lattice. If, for example, at $\theta=0°$ we project all the particles on the direction of the wave propagation, the distance between these projections will be $a/2$. The spectrum in this case [Figs. 2(a),(e)] extends up to $ka=2\pi$. Another periodic spectrum is produced at $\theta=30°$. The particle projections are spaced by $\sqrt{3}a/2$ producing a spectrum [Figs. 2(d),(h)] up to $ka=2\pi/\sqrt{3}$. This spectrum is identical to the one for a linear chain [14] with particle separation $\sqrt{3}a/2$. For a wave propagating in an arbitrary direction, the separation of the particle projections can be infinitely small (for an infinite lattice) and therefore infinitely small wavelengths can be sustained, producing aperiodic phonon spectra. The spectra for $\theta=10°$ [Figs. 2(b),(f)] and $\theta=20°$ [Figs. 2(c),(g)] are aperiodic, at least in the first and second Brillouin zones.

Our theory divides the phonon spectra (Fig. 2) into two branches: high frequency ω_h (short dashes) and low frequency ω_l (long dashes). This is different from the standard approach which differentiates only between longitudinal and transverse modes. The reason for this is illustrated in Figs. 2(i)–(l), which show the spectrum for $\theta=15°$. The total spectrum [Fig. 2(i)] has two branches: high and low frequency. We plotted the parts of this spectrum corresponding to the longitudinal [Fig. 2(j)] and transverse [Fig. 2(k)] polarization (mode) separately. The branches break, indicating that the polarization alternates between longitudinal and transverse. The polarization P, calculated from the theory, is plotted in Fig. 2(l). As mentioned earlier, $P=1$ indicates that the wave is longitudinal. The waves are purely longitudinal or transverse only in the long-wavelength regime ($ka\lesssim\pi$). For $ka\gtrsim\pi$ the waves have mixed polarization. Mixed polarization means that the individual particles do not move just along or across the wave vector. It implies that the particles move on elliptical orbits or on lines inclined to the direction of propagation.

The data at $\theta=0°$ [Figs. 2(a),(e)] reproduce the result of Ref. [11] and extend it into the shorter wavelengths (larger wave numbers k). There is no mixed polarization in the case of a wave propagating along one of the main axes. The high frequency branch is longitudinal and the low frequency branch is transverse up to their crossing point. Then the ω_h branch becomes transverse and the ω_l branch becomes longitudinal up to the next crossing point, where they change polarizations back again. This corresponds to the known longitudinal and transverse modes [6,9–12]. If the wave propagates along the second main axis at $\theta=30°$, the high frequency branch is always longitudinal and the low frequency branch is always transverse. The dispersion relation for $ka\ll\pi$ (long wavelengths) is identical for all angles of propagations.

In summary, we obtained the phonon spectra of a 2D Yukawa lattice experimentally, theoretically, and using a molecular dynamics simulation for different angles of propagation with respect to the crystal axes. All three results well agree with each other. It is found that the spectra are isotropic for long wavelengths and highly anisotropic for short wavelengths. The waves have a pure longitudinal or transverse polarization only if they propagate along one of the main crystal axes or have a long wavelength. They have a mixed polarization for an arbitrary direction of propagation.

We thank U. Konopka and R. Quinn for useful discussions. S.N. acknowledges the Japan Society of the Promotion of Science.

[1] H. Ikezi, Phys. Fluids **29**, 1764 (1986).
[2] H. Thomas, G. Morfill, V. Demmel, J. Goree, B. Feuerbacher, and D. Möhlmann, Phys. Rev. Lett. **73**, 652 (1994).
[3] Y. Hayashi and K. Tachibana, Jpn. J. Appl. Phys., Part 2 **33**, L804 (1994).
[4] J. Chu and I. Lin, Phys. Rev. Lett. **72**, 4009 (1994).
[5] H. Thomas and G. Morfill, Nature (London) **379**, 806 (1996).
[6] F. Peeters and X. Wu, Phys. Rev. A **35**, 3109 (1987).
[7] D.H.E. Dubin, Phys. Plasmas **7**, 3895 (2000).
[8] X. Wang, A. Bhattacharjee, and S. Hu, Phys. Rev. Lett. **86**, 2569 (2001).
[9] S. Nunomura, D. Samsonov, and J. Goree, Phys. Rev. Lett. **84**, 5141 (2000).
[10] S. Nunomura, J. Goree, S. Hu, X. Wang, and A. Bhattacharjee, Phys. Rev. E **65**, 066402 (2002).
[11] S. Nunomura, J. Goree, S. Hu, X. Wang, A. Bhattacharjee, and K. Avinash, Phys. Rev. Lett. **89**, 035001 (2002).
[12] S.K. Zhdanov, D. Samsonov, and G.E. Morfill, Phys. Rev. E **66**, 026411 (2002).
[13] D. Samsonov, A. Ivlev, R. Quinn, G. Morfill, and S. Zhdanov, Phys. Rev. Lett. **88**, 095004 (2002).
[14] F. Melandsø, Phys. Plasmas **3**, 3890 (1996).